

# Polyhedral Shapes of CeO<sub>2</sub> Nanoparticles

Zhong Lin Wang<sup>\*,†</sup> and Xiangdong Feng<sup>‡</sup>

School of Materials Science and Engineering, Georgia Institute of Technology, Atlanta, Georgia 30332-0245, and Technology Center, Ferro Co., 7500 E. Pleasant Valley Rd., Independence, Ohio 44131

Received: September 19, 2003

Ceria nanoparticles are a widely used nanomaterial for applications in catalysts, fuel cell, and microelectronics. An important factor that influences the performance of CeO<sub>2</sub> is the particle shape. In this paper, a systematic study has been carried out to determine the shapes of CeO<sub>2</sub> nanoparticles. For particles in the size range of 3–10 nm, the particle shape is dominated by truncated octahedral that is defined by the {100} and {111} facets. The fastest growth of the nanoparticles along <100> results in the disappearance of the {100} facets; thus, the large size CeO<sub>2</sub> particles are dominated by the octahedral shape with flat surfaces. The nanoparticles agglomerate by minimizing the interface energy with the formation of a lattice matched “coherent interface”. The faceted shape also results in the textured distribution of nanoparticles deposited onto a substrate surface, with a preferred orientation of [110]. These structural characteristics are likely to affect their performance in technological applications.

## 1. Introduction

Ceria nanoparticles are one of the most important nanomaterials for a wide range of applications in catalysts,<sup>1,2</sup> fuel cell,<sup>3</sup> chemical–mechanical polishing for microelectronics, phosphor/luminescence,<sup>4</sup> and metallurgical and glass/ceramic applications. These applications are mainly based on cerium’s high thermodynamic affinity for oxygen and sulfur, its potential redox chemistry involving Ce(III)/Ce(IV), and absorption/excitation energy bands associated with its electronic structure. The size and size distribution of ceria are important in determining their properties.<sup>5</sup>

The chemical approach is the main route for synthesis of CeO<sub>2</sub> nanoparticles.<sup>6,7</sup> It is known that nanoparticles usually have specific shape, especially when they are small, because a single-crystal nanoparticle has to be enclosed by crystallographic facets that have lower energy; a spherical particle usually has higher surface energy due to the presence of high index crystallographic facets. Although a large effort has been devoted to studying the shapes of metallic nanoparticles, there is few report about the detailed surface structure of CeO<sub>2</sub> nanoparticles. This paper aims at studying the shapes of CeO<sub>2</sub> nanoparticles of different sizes using high-resolution transmission electron microscopy (HRTEM). After a brief introduction on the experimental method, the experimental results provided by HRTEM will be presented. The shape of the small-sized CeO<sub>2</sub> nanoparticles is dominated by truncated octahedron defined by the {100} and {111} facets, while the large-sized CeO<sub>2</sub> particles are defined by the {111} enclosed octahedral, indicating fast growth along <100> during the growth. Then, the interface between nanoparticles is investigated to understand the textured orientation of the nanoparticles while forming an aggregate, and the result will be explained on the basis of the shape of the particles.

## 2. Experimental Method

The CeO<sub>2</sub> nanoparticles were synthesized through a hydrothermal process. Cerium ammonia nitrate was dissolved in water, and ammonia hydroxide solution was added to precipitate the cerium salt. A milky slurry was formed and was heated at 300 °C for 2–6 h. The resulting nanoparticles were decanted and washed several time with water. The secondary particle size was measured using a light scattering technique on a submicron particle sizer (NICOMP 380), and the mean particle size was 98 nm. The X-ray diffraction analysis of the as-synthesized samples using a Philips APD 3720 system showed the typical CeO<sub>2</sub> structure with CaF<sub>2</sub> lattice.

The as-synthesized nanoparticles were suspended in solution, a droplet of which was deposited on a TEM grid covered with a carbon film. After drying in air, the nanoparticles are collected on a carbon substrate for TEM analysis. Crystallographic and surface structures of CeO<sub>2</sub> particles were determined by HRTEM, performed using an JEOL 4000EX transmission electron microscope (TEM) operated at 400 kV. This TEM is ideally suited for high-resolution structural imaging at a point-to-point Schertzer image resolution better than 0.18 nm.

## 3. Experimental Results and Discussions

**3.1. Shapes of Small-Sized CeO<sub>2</sub> Nanoparticles.** The first part of this study focuses on the nanoparticles that are of sized in the range 3–10 nm. Figure 1a shows a low-magnification TEM image of the CeO<sub>2</sub> nanoparticles, displaying a fairly uniform size distribution and the agglomeration of the nanoparticles. The average particle size is ~6 nm. The electron diffraction pattern recorded from the area can be indexed according to the CaF<sub>2</sub>-type structure.

The shapes of the CeO<sub>2</sub> nanoparticles have been systematically analyzed by high-resolution TEM. By recording a large amount of images from unselected areas and identifying the lattice fringes and particle orientation, the facets on the particle surfaces have been determined. A few typical images from the nanoparticles are displayed in Figure 2. The dominant lattice

\* Corresponding author. E-mail: zhong.wang@mse.gatech.edu.

<sup>†</sup> Georgia Institute of Technology.

<sup>‡</sup> Ferro Co.

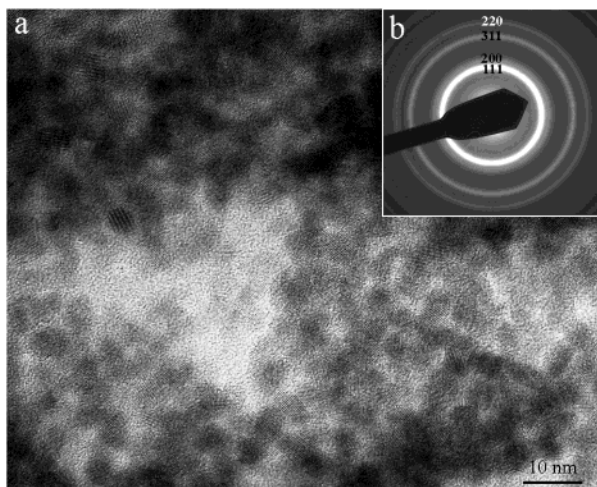


**Figure 1.** A low-magnification TEM image of the small-sized  $\text{CeO}_2$  nanoparticles and the corresponding electron diffraction pattern.

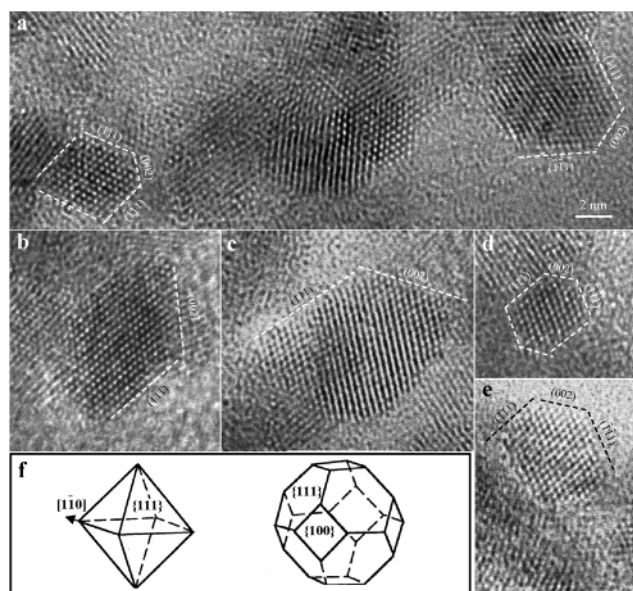


**Figure 2.** (a–e) Typical high-resolution TEM images of  $\text{CeO}_2$  nanoparticles oriented along  $[110]$ , showing the facet structures as defined by the  $\{002\}$  and  $\{111\}$  facets. (f) Structural models of the octahedral and truncated octahedral shapes.

fringes are the  $\{111\}$  and  $\{002\}$ , which are observed when the particles are oriented along  $[110]$ . Due to the agglomeration of the particles, caution needs to be exercised in identifying that the fringes are from the lattices of the same crystal rather than the intersections between the atomic planes belonging to two overlapped crystals. Figure 2a–e shows a few nanoparticles that are oriented along  $[110]$ , along which the  $(111)$ ,  $(\bar{1}\bar{1}\bar{1})$ , and  $(002)$  lattice planes are imaged edge-on. The labeling of the observed crystal planes for these nanoparticles is indicated in the figure. Each nanoparticle is a single crystal and there is no twin or stacking fault. On the basis of the information provided by these images, the shapes of the particles are constructed. There are two types, one is the octahedral enclosed by eight  $\{111\}$  planes, and the other is the truncated octahedral enclosed by eight  $\{111\}$  and six  $\{100\}$  planes, as shown in Figure 2f. The  $[110]$  direction is along a side edge of the polyhedron, as indicated by an arrowhead. Particles presented here are the truncated octahedral, which are more “spherical-like”.

Figure 3a shows three particles that are rather spherical, but a careful analysis can index the atomic lattices to be the  $\{111\}$

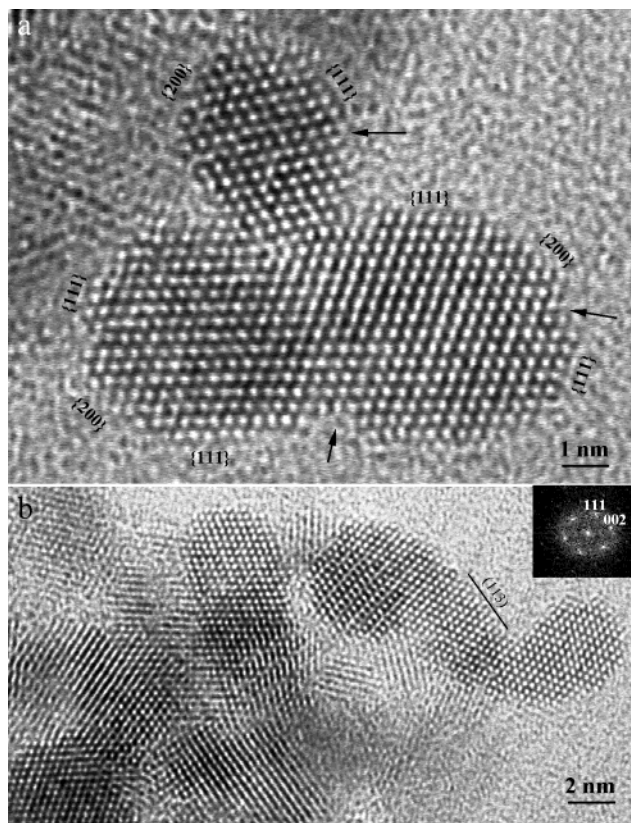


**Figure 3.** (a, b) High-resolution TEM images of  $\text{CeO}_2$  nanoparticles oriented along  $[110]$  with “spherical-like” and irregular shapes, respectively. The inset in panel b is a Fourier transform of the HRTEM image from the irregular shape nanoparticle.

and  $\{200\}$ . These particles have a clean surface and there is no passivation. Thus, when they are in contact, the lattices from the two particles tend to align. There are some point defects on the surfaces, which are indicated by arrowheads for the missing atomic rows. This is expected because the synthesis temperature was low and there is not enough energy for the particle to achieve equilibrium shape. Figure 3b shows a couple of irregularly shaped nanoparticles, some  $\{111\}$  and  $\{200\}$  (or equivalently  $\{100\}$ ) facets can be identified, but a high-index facet such as  $(113)$  can also be identified. These types of particles are likely to have higher energy than the spherical-like particles.

As a summary of the above observation, the  $\{200\}$  and  $\{111\}$  enclosed truncated-octahedral is the most popular shape. To understand this result, we start from the unit cell structure of  $\text{CeO}_2$  (Figure 4a). The unit cell of  $\text{CeO}_2$  is made of a face-centered cubic (fcc) structured Ce lattice and a cubic oxygen cage located inside the fcc cation lattice.<sup>8</sup> Naturally, this structural configuration may have some similarity to the fcc lattice. From the structure model for the  $(100)$ ,  $(110)$ , and  $(111)$  planes, shown in parts b, c, and d of Figure 4, respectively, the surface density of atoms in the corresponding planes follows  $n_{(111)} > n_{(200)} > n_{(110)}$ . For a fcc structured metal, the surface energy for the three lowest index planes follows:  $\gamma_{\{111\}} < \gamma_{\{200\}} < \gamma_{\{110\}}$ .<sup>9</sup> The above experimental data suggest that this rule may also hold for  $\text{CeO}_2$ .

**3.2. Shape of Large-Sized  $\text{CeO}_2$  Particles.** For the samples that are dominated by large-sized  $\text{CeO}_2$  particles, facets are apparent from the scanning electron microscopy (SEM) images (Figure 5a and b). The particles are well-defined and the agglomeration between the particles also exists. The particles tend to share common faces in order to maximize the packing



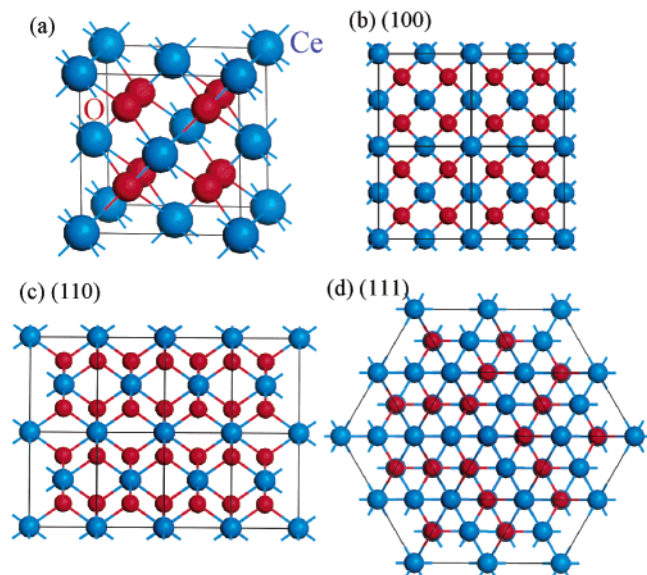


**Figure 4.** (a) Unit cell of the CeO<sub>2</sub> structure. (b–d) The (100) [or (200)], (110), and (111) planes of the CeO<sub>2</sub> structure.

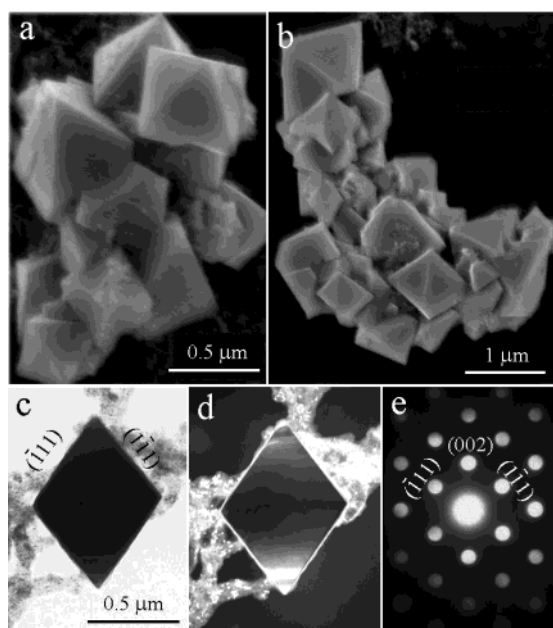


**Figure 5.** (a, b) SEM image of large-sized CeO<sub>2</sub> particles, showing an octahedral shape. (b, c, d) Bright-field and dark-field TEM images of an octahedral particle and the corresponding electron diffraction pattern, respectively.

density. This is a general principle in forming a self-assembled nanostructure. The facet structure of the particles is determined by TEM. Due to the large thickness of the particle, the bright-field TEM image is rather dark, while the dark-field image shows some change in sample thickness from the top to the bottom (Figure 5c,d). Electron diffraction shows that the facets are {111}, and the particle is oriented along [110]. The particle shape matches very well to the octahedral presented in Figure 2f.

An evolution in particle shape from truncated octahedral to octahedral is due to the shrinkage of the {200} surfaces. This is possible only if the growth rate along the <100> is much faster than that along <111>. The formation of the octahedral is due to the lowest energy of the {111} surfaces.

**3.3. Coherent Interface.** Agglomeration of nanoparticles is a very common phenomenon that occurs because the nanopar-

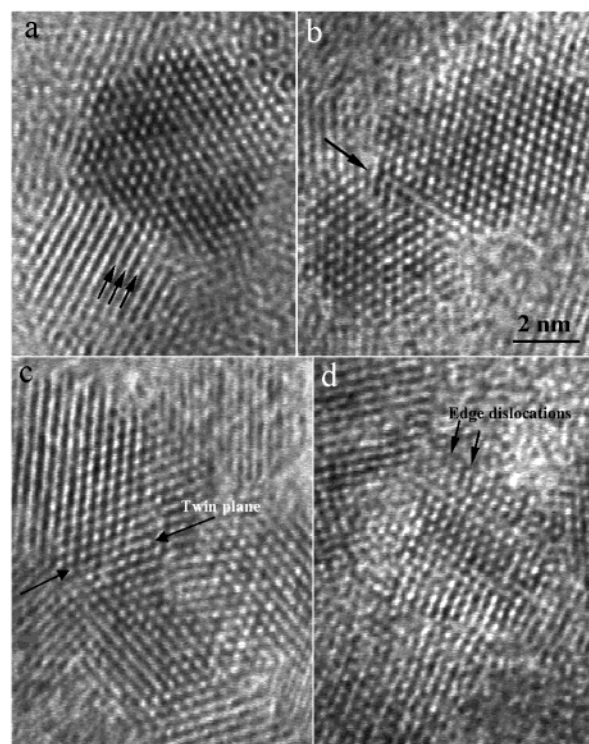


**Figure 6.** High-resolution TEM images of CeO<sub>2</sub> nanoparticles oriented along [110], displaying (a, b) the coherent match at the interfaces between the particles, (c) a twin boundary, and (d) edge-dislocations near the surface.

ticles tend to decrease the exposed surface in order to lower the surface energy. When two particles are in contact, due to the existence of mismatch between the lattices, the two crystals tend to rotate with each other to minimize the interface strain energy. For two sets of crystal planes that are oriented in parallel, the interface strain is  $\epsilon \approx |d_1 - d_2|/d_1$ , where  $d_1$  and  $d_2$  are the interplanar distances for the two sets of planes, respectively. The interface energy is minimized if  $d_1 = d_2$ , which means that the same type of planes, such as {111}, tend to align with each other, forming a coherent interface. This situation is clearly presented by the three particles displayed in Figure 3a. For a general case, the results presented in Figure 6 are what we have expected.

The two nanoparticles in Figure 6a have a matched (111) plane, although there is a twist parallel to the plane so that one nanoparticle is oriented along  $[\bar{1}\bar{1}0]$  while the other one is slightly off the zone axis. The two nanoparticles in Figure 6b have the same  $[\bar{1}\bar{1}0]$  orientation, but there is a small relative twist; thus, the atoms at the interfacial region have to be strained to accommodate the local deformation, as indicated by an arrowhead. In some cases, a twin boundary is formed between the two particles (Figure 6c), which tend to have lower energy than the conventional grain boundary. Edge type of dislocations may also be identified near the surface of the nanocrystal, as indicated by arrowheads in Figure 6d.

As a result of minimizing interface energy, the particles tend to form a coherence interface, leading possibly to a preferred orientation in particle orientation. Figure 7a shows a typical HRTEM image recorded from a group of particles in which a large fraction of the particles show the {111} lattice fringes and the preferred [110] orientation. The formation of this “textured” structure is also related to the shape of the particles. Figure 7b shows two particles that are oriented in the same [110] direction and share a common (111) face. This type of close

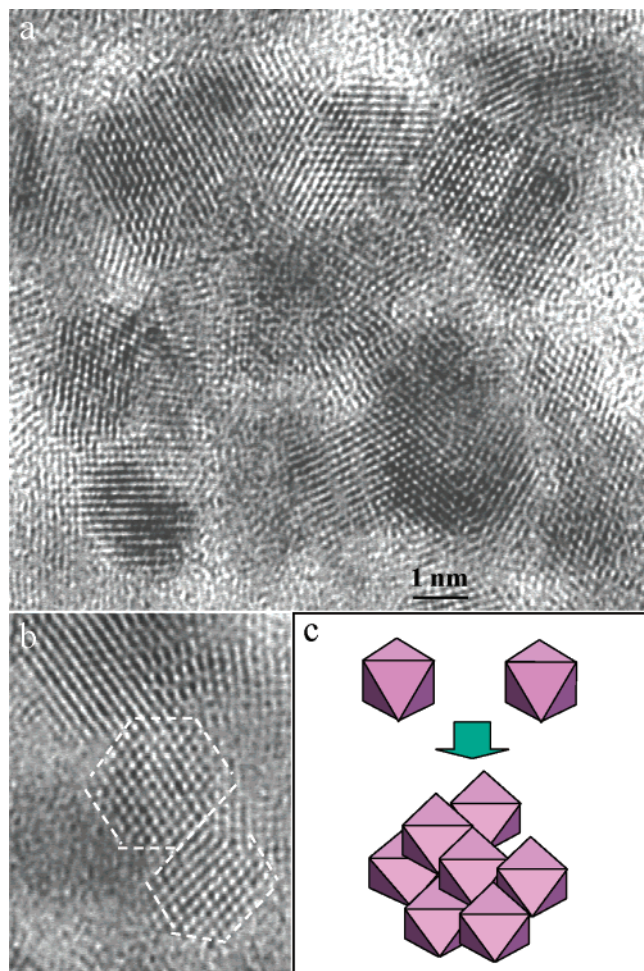


**Figure 7.** (a) High-resolution TEM images of CeO<sub>2</sub> nanoparticles, showing their [110] preferred orientation and textured structure. (b) Two particles with face-to-face contact and coherent interfacial matching. (c) Polyhedral model showing the configuration of nanoparticle assembly.

packing is the reason for forming the textured structure, as explained below.

Our analysis in section 3.1 indicates that the nanoparticles have an octahedral or truncated octahedral shape. For simplicity of illustration, we use a polyhedron in octahedral shape. The stacked octahedrals tend to share the same type of faces (Figure 7c), such as {111} to {111} or {200} to {200}, which has the

smallest interface mismatch and thus the minimized interface energy. Therefore, the two octahedra prefer to align, forming a preferred orientation in particle distribution. A textured agglomeration is formed if a number of particles are stacked together by following a face-to-face packing as well as the coherent interface (Figure 7c).

#### 4. Conclusion

Using high-resolution TEM, a systematic study has been carried out to determine the shapes of CeO<sub>2</sub> nanoparticles for different sizes. For particles in the size range of 3–10 nm, the particle shape is dominated by a truncated octahedral that is enclosed by the {100} and (111) facets. As the particles grow larger, the fastest growth of the nanoparticles along <100> results in the disappearance of the {100} facets; thus, the larger size CeO<sub>2</sub> particles are dominated by the octahedral shape with flat surfaces.

Due to the uncapped surfaces, the nanoparticles agglomerate by minimizing the interface energy with the formation of a lattice-matched “coherent interface”. As a result, the faceted shape also results in the textured distribution of nanoparticles deposited onto a substrate surface, with a preferred orientation of [110]. These structural characteristics are likely to affect their performance in technological applications.

**Acknowledgment.** Thanks to Jackie Davis for particle synthesis experiments, Dave Gnizak for SEM photos of the particles, and Dr. Xiangyang Kong his help in manuscript preparation.

#### References and Notes

- (1) Bera, P.; Hegde, M. S. *Catal. Lett.* **2002**, *79*, 75.
- (2) Valenzuela, R. X.; Bueno, G.; Solbes, A.; Sapina, F.; Martinez, E.; Corberan, V. C. *Topics Catal.* **2001**, *15*, 181.
- (3) Kang, Z. C.; Wang, Z. L. *Adv. Mater.* **2003**, *15*, 521.
- (4) Yu, X. J.; Xie, P. B.; Su, Q. D. *Phys. Chem. Chem. Phys.* **2001**, *3*, 5266.
- (5) Spanier, J. E.; Robinson, R. D.; Zheng, F.; Chan, S. W.; Herman, I. P. *Phys. Rev. B* **2001**, *64*, 245407.
- (6) Feng, X. D.; Hu, M. Z. In *Encyclopedia of Nanoscience and Nanotechnology*; Nalwa, H., Ed.; American Scientific Publishers: 2003; in press.
- (7) Adschiri, T.; Hakuta, Y.; Sue, K.; Arai, K. *J. Nanoparticle Res.* **2001**, *3*, 227.
- (8) Wang, Z. L.; Kang, Z. C.; *Functional and Smart Materials—Structural Evolution and Structure Analysis*; Plenum Publishing Co.: New York, 1998; Chapter 4.
- (9) Wang, Z. L. *J. Phys. Chem. B* **2000**, *104*, 1153.